Journal of Medicinal Chemistry

Article

pubs.acs.org/jmc

Enantioselective Synthesis and in Vivo Evaluation of Regioisomeric Analogues of the Antimalarial Arterolane

Brian R. Blank,[†] Jiri Gut,[‡] Philip J. Rosenthal,[‡] and Adam R. Renslo*[,†]

[†]Department of Pharmaceutical Chemistry and [‡]Department of Medicine, University of California San Francisco, 1700 Fourth Street, San Francisco, California 94158, United States

Supporting Information

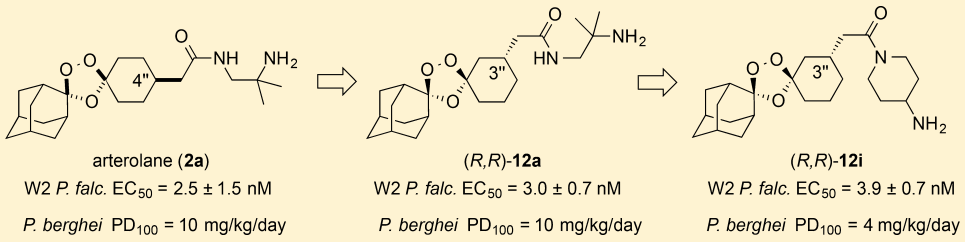

ABSTRACT: We describe the first systematic study of antimalarial 1,2,4-trioxolanes bearing a substitution pattern regioisomeric to that of arterolane. Conformational analysis suggested that *trans*-3″-substituted trioxolanes would exhibit Fe(II) reactivity and antiparasitic activity similar to that achieved with canonical *cis*-4″ substitution. The chiral 3″ analogues were prepared as single stereoisomers and evaluated alongside their 4″ congeners against cultured malaria parasites and in a murine malaria model. As predicted, the *trans*-3″ analogues exhibited in vitro antiplasmodial activity remarkably similar to that of their *cis*-4″ comparators. In contrast, efficacy in the *Plasmodium berghei* mouse model differed dramatically for some of the congeneric pairs. The best of the novel 3″ analogues (e.g., **12i**) outperformed arterolane itself, producing cures in mice after a single oral exposure. Overall, this study suggests new avenues for modulating Fe(II) reactivity and the pharmacokinetic and pharmacodynamic properties of 1,2,4-trioxolane antimalarials.

INTRODUCTION

Despite recent progress in the control and treatment of malaria, this devastating disease still affects millions around the world and was estimated by the World Health Organization to have caused 429,000 deaths in 2015. The blood stage of infection is responsible for symptomatic disease, which is characterized by cyclical rounds of asexual replication of Plasmodium spp. parasites within host erythrocytes. To support its rapid proliferation in this stage of infection, the parasite depends on the catabolism of host hemoglobin as a source of amino acids. However, the consequent production of toxic free ferrous iron heme during this process represents an Achilles heel that is targeted in different ways by multiple classes of approved antimalarials, including quinolines and artemisinins.

The sesquiterpene artemisinin (qinghaosu, **1**) and its analogues dihydroartemisinin (DHA) and artesunate are employed in artemisinin-based combination therapies (ACT), the current WHO recommended front line therapy for uncomplicated malaria caused by *Plasmodium falciparum*, the most virulent human malaria parasite. Artemisinins exhibit a novel pharmacology that requires initial activation of a hindered endoperoxide bond by reduced iron sources in the parasite. The iron-dependence and likely involvement of carbon-centered radical intermediates in artemisinin pharmacology were first revealed in the early 1990s in elegant mechanistic work involving synthetic artemisinin derivatives.[1,2] Soon, more synthetically accessible chemotypes were identified that, like the artemisinins, bore a peroxide bond in a sterically hindered environment. Most notably, Vennerstrom and co-workers identified the 1,2,4-trioxolane-based pharmacophore that produced both arterolane[3] (OZ277, **2a**) and artefenomel[4] (OZ439, **3**) (Figure 1). Clinical development of arterolane by Ranbaxy led to its approval in India and some African countries as a combination with piperaquine. Artefenomel was subsequently selected for clinical development

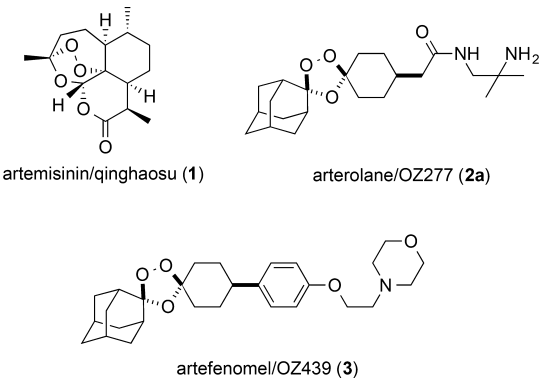

Figure 1. Structures of antimalarial endoperoxides.

Received: May 11, 2017

DOI: 10.1021/acs.jmedchem.7b00699
J. Med. Chem. XXXX, XXX, XXX−XXX

on the basis of its much superior Fe(II) stability and in vivo PK/PD properties[5] and is currently in Phase 2 clinical trials.[6]

Recent chemoproteomic studies[7−9] from two different groups have confirmed the long-hypothesized pleiotropic action of the artemisinins and demonstrated[7] a remarkable concordance in the proteins covalently targeted by artemisinins and synthetic 1,2,4-trioxolanes. Hence, artemisinin and 1,2,4-trioxolane-derived affinity probes were shown to irreversibly label numerous proteins in the parasite, including those involved in energy acquisition, antioxidant response, and protein and DNA synthesis. Yet despite having many potential targets in the parasite, resistance to artemisinins has emerged in Southeast Asia and is now a significant clinical problem, especially with concomitant resistance to partner drugs.[10] The resistant phenotype results from mutations in the propeller domain of the PfKelch13 (K13) protein, which shares homology with the mammalian Keap1 protein.[11] These mutations appear to confer an enhanced stress response and a prolonged ring stage that allows K13 mutant parasites to better sustain the potent but short-lived insult conferred by artemisinins.[12]

A number of groups have now explored whether K13 mutations confer resistance also to antimalarial 1,2,4-trioxolanes, employing in vitro assays that focus on the kinetics of ring-stage killing. Thus, Tilley and co-workers[13] studied killing kinetics of DHA, **2a**, and **3** against a clinical K13 mutant strain and a genetically matched K13 revertant strain bearing the wild-type K13 allele. For all three agents, the time to reduce early ring viability by 50% ($t^{\wedge}_{50}$) was more than doubled in the K13 mutant strain compared to that in the revertant parasites. Thus, DHA and **2** exhibited $t^{\wedge}_{50}$ values of ∼3 and ∼1 h for the K13 mutant and revertant strains, respectively, whereas **3** exhibited slower killing with $t^{\wedge}_{50}$ values of ∼5 and ∼2 h. Using a ring-stage survival assay and a larger panel of K13 mutants, Fidock and co-workers[14] found that DHA and **2a** were uniformly less effective against the K13 strains when compared to revertant or wild-type controls. In contrast, compound **3** showed cross-resistance to only one of the K13 mutants examined (I543T). Finally, Wittlin and co-workers[15] studied clinical (**2a**, **3**) as well as additional preclinical trioxolane analogues against a K13 clinical isolate, finding that the synthetic trioxolanes were superior to DHA in a ring stage survival assay. Although the findings of these three studies are in some cases at odds, they are in general agreement that structurally distinct endoperoxide antimalarials can exhibit divergent effects on K13 mutant rings and that the superior in vivo exposure profile of **3** in humans predicts for efficacy in patients with K13 mutant parasites. Early data[6] from the clinical investigation of **3** suggests this is indeed the case.

The findings summarized above provide essential guidance for the optimization of endoperoxide antimalarials in the current environment of K13-mediated resistance. New agents should ideally confer rapid killing of wild-type and mutant K13 parasites while retaining a prolonged in vivo exposure profile that ideally enables single-dose therapy.[9,13] Among currently available agents, **3** meets this pharmacokinetic (PK) target, whereas **2a** and current artemisinins do not due to shorter durations of exposure in vivo. The identification of novel 1,2,4-trioxolanes that combine rapid ring-stage killing kinetics with superior pharmacokinetics will be expedited by new approaches for the control of endoperoxide reduction/activation by Fe(II). Here, we provide data suggesting that *trans*-3″-substitution of the cyclohexane ring, like canonical *cis*-4″ substitution, modulates Fe(II) reactivity of 1,2,4-trioxolanes in a pharmacologically relevant regime in vivo. Comparing congeneric sets of *trans*-3″ and *cis*-4″ analogues, we furthermore demonstrate that *trans*-3″ analogues can exhibit in vivo PK/PD properties distinct from *cis*-4″ comparators. Finally, we describe an efficient and stereocontrolled synthesis of *trans*-3″-substituted 1,2,4-trioxolane analogues that will enable further lead optimization studies of this chemotype.

RESULTS AND DISCUSSION

Design and Synthesis. The Fe(II) reactivity and resulting antimalarial effects of **2a** and **3** can be rationalized in terms of the conformational dynamics of the cyclohexane ring. In ground state conformer I (Scheme 1), the axial endoperoxide lies in the concave face of an aliphatic surface with approach to the σ* orbital of the O−O bond effectively shielded by the four proximal axial hydrogen atoms of the adamantane and cyclohexane rings (Scheme 1). It is the peroxide-equatorial conformer II that exposes the O−O bond for inner-sphere coordination with Fe(II) and single-electron transfer leading to bond scission.[16] Consistent with this interpretation is the highly regioselective nature of peroxide cleavage with reaction at the oxygen atom opposite the adamantane moiety predominating (O^1, Scheme 1).[16] The crucial role of cyclohexane ring conformation on Fe(II) reactivity allows the latter to be finely tuned by varying the nature and stereochemistry of the 4″ substituent (i.e., R^4 in Scheme 1).[16] The optimal balance of Fe(II) reactivity and antiplasmodial effects was ultimately achieved in analogues bearing *cis*-R^4 substitution that stabilizes unreactive conformer I. A focus on *cis*-R^4 substitution during lead optimization efforts ultimately produced both of the clinical candidates from this class (**2a** and **3**). Moreover, the improved stability of $\mathbf{3}^4$ as compared to **2a** toward endogenous Fe(II) sources can be understood as arising from more severe 1,3-diaxial interactions in conformer II of compound **3** due to the bulkier aryl R^4 side chain. Importantly, **3** still retains sufficient reactivity with free Fe(II) heme in parasites to confer a potent antimalarial effect.

Scheme 1. Conformational Effects on Fe(II) Reactivity in Antimalarial 1,2,4-Trioxolanes

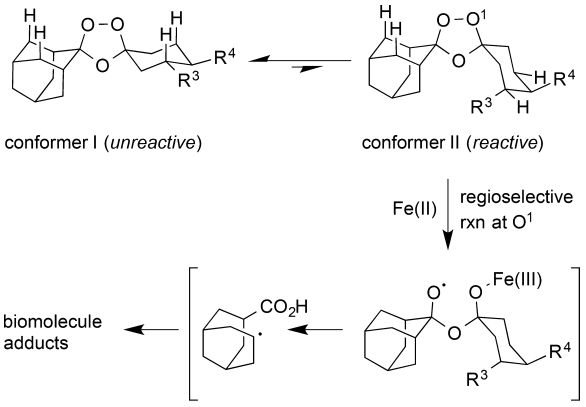

The ability to predict Fe(II) reactivity on conformational grounds is very appealing from a design perspective and may prove essential in finding the right balance of in vivo stability toward endogenous Fe(II) sources (principally labile iron) and reactivity with Fe(II) heme necessary to target both susceptible and resistant parasites. We considered that *trans*-3″ substitution, nearly[17] unexplored previously, should modulate conformational dynamics in an analogous fashion as canonical *cis*-4″ substitution (R^3 vs R^4, Scheme 1). In the case of *trans*-R^3 analogues, however,

DOI: 10.1021/acs.jmedchem.7b00699
J. Med. Chem. XXXX, XXX, XXX−XXX

1,3-diaxial interactions in conformer II would involve both O and H atoms as opposed to only H atoms in *cis*-R^4 analogues. Depending on the nature of the R^3/R^4 side chain then, distinct conformational dynamics of the cyclohexane ring might be expected, and this would confer distinct in vitro and in vivo activities. Other important properties such as solubility, metabolism, and clearance were also expected to be affected by the switch to *trans*-R^3 substitution, which eliminates the internal symmetry present in **2a** and **3**, producing a distinct topology.

The arterolane (**2a**) scaffold was selected for initial studies because a late-stage amide coupling reaction would allow ready access to the matched R^3/R^4 analogue pairs. As comparators, we selected several R^4-side chain derivatives described in patent applications[18] and reported to possess reasonable in vivo efficacy with oral dosing. Thus, **2a** and nine additional R^4-side chain analogues (**2b–j**) were synthesized[19] from acid intermediate **4**[17] and commercially available amines (Scheme 2). We then turned our attention to construction of the analogous R^3-side chain variants.

Scheme 2. Synthesis of Arterolane and Related *cis*-4″ Analogues from Key Intermediate 4[a]

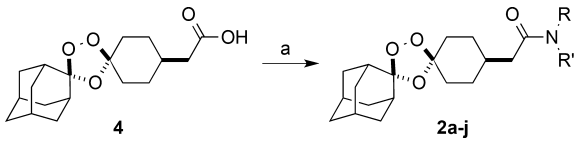

[a]Reagents and conditions: (a) ethyl chloroformate, Et_3N, CH_2Cl_2, −10 °C, 75 min; R(R′)NH, CH_2Cl_2, −10 °C to rt, 2–24 h, 71–95%. Reaction conditions adapted from ref 19.

Unlike in analogues **2a–j**, which possess internal symmetry and are achiral, R^3 substitution leads to four possible stereoisomers. Because *trans*-R^3 stereochemistry was desired based on our conformational analysis, this left the *trans*-(*R*,*R*) and *trans*-(*S*,*S*) enantiomers as potential candidates for evaluation. We arbitrarily selected the *trans*-(*R*,*R*) stereoisomers for this initial study. Previously, we found[20] that the Griesbaum co-ozonolysis reaction of 3-substituted cyclohexanones proceeds with high (~90:10 dr) intrinsic diastereoselectivity and favors the desired *trans* stereoisomer. Preparing the desired *trans*-(*R*,*R*) stereoisomer then required starting from an appropriate nonracemic 3-cyclohexanone. Toward this end, cyclohexanone **5** was prepared in 87% yield via catalytic asymmetric Michael addition of dimethyl malonate to 2-cyclohexen-1-one (Scheme 3).[21−23] Notably, this very practical synthesis of **5** has been performed previously on kilogram scales in a premanufacturing setting.[23] We confirmed the high enantiomeric purity of **5** (95% ee) by conversion to ketal **6**,[24,25] the two diastereomers of which could be readily distinguished by ^{13}C NMR spectroscopy.

A Krapcho decarboxylation was next considered as a means to produce the desired ester **7**[26] from **5**. However, for the possibility of epimerization via retro-Michael/Michael addition of dimethyl malonate to be avoided, a two-step procedure was utilized instead.[26] Thus, hydrolysis of **5** with NaOH at 0 °C afforded the mono-carboxylate intermediate, which was immediately heated to 160 °C to facilitate decarboxylation. This afforded **7** in 85% yield over two steps. Conversion of **7** to ketal **8** confirmed that the hydrolysis/decarboxylation sequence had proceeded without erosion of enantiomeric purity (94% ee for **7**). Griesbaum co-ozonolysis of **7** with two equivalents of oxime **9** at 0 °C using our optimized conditions[20] afforded 1,2,4-trioxolane intermediate **10**

Scheme 3. Enantiocontrolled Synthesis of Ketone 7[a]

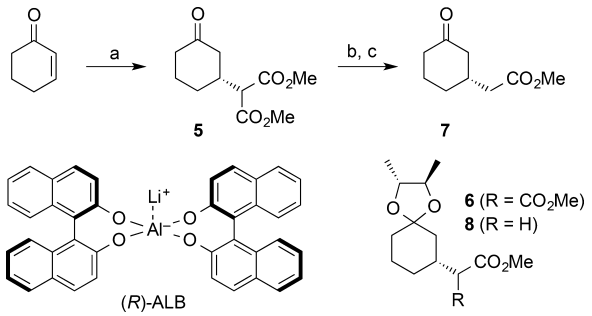

[a]Reagents and conditions: (a) dimethyl malonate, (*R*)-ALB (1 mol %), *t*-BuOK (0.9 equiv relative to ALB), 4 Å MS, THF, rt, 68 h, 87%; (b) NaOH, H_2O/THF (11:1), 0 °C, 2 h; (c) DMSO, 160 °C, 4 h, 85% over two steps.

in nearly quantitative yield. Hydrolysis of ester **10** with NaOH then furnished the desired carboxylic acid **11** in excellent yield. From **11**, the desired 3″ amides **12a–k** were prepared in 68–95% yields via formation of the mixed anhydride (ethyl chloroformate and Et_3N at −10 °C) and subsequent reaction with primary or secondary amines (Scheme 4). We were able to confirm that the Griesbaum co-ozonolysis of **7** and **9** had proceeded with good diastereoselectivity (91:9 dr) by the preparation of analogue **12k** in which trans and cis diastereomers could be readily distinguished by NMR.[20]

In Vitro Evaluation of Congener Pairs. The effect of R^3 substitution on antiplasmodial activity was evaluated by comparing the regioisomeric analogues **2a–j** and **12a–j** (Chart 1). New *trans*-R^3 analogues exhibited potent, low nM activities against the chloroquine-resistant W2 strain of *P. falciparum* with activity comparable to that of *cis*-R^4 comparators. Moreover, structure–activity trends tracked remarkably closely in the regioisomeric scaffolds consistent with our hypothesis that *trans*-R^3 substitution should confer similar conformational constraints and Fe(II) reactivity as *cis*-R^4 substitution. In both scaffolds, piperidine amides (**12e** and **2e**) were the least potent, approximately 10- to 20-fold weaker than piperazine analogues **12g** and **2g**. The most significant difference between regioisomer pairs was observed for morpholine amides **12f** and **2f**, where 3″ analogue **12f** was 3-fold more potent than that of **2f**. Overall, these findings confirmed that *trans*-R^3 substitution modulates 1,2,4-trioxolane reactivity in a pharmacologically relevant range, producing effects on cultured parasites that are comparable to those of canonical *cis*-R^4 substitution.

A second hypothesis regarding *trans*-R^3 substitution was that the resulting desymmetrized molecular topology would impact the in vivo PK/PD properties of these analogues. Specifically, we reasoned that the chiral *trans*-R^3 analogues might interact differently with CYP enzymes and drug transporters (e.g., P-gp). To explore possible metabolic differences, we evaluated selected analogues with mouse liver microsomes and derived intrinsic clearance (CL_{int}) values (Table 1). All the analogues evaluated exhibited low or moderate CL_{int} values that would predict reasonable exposure in vivo. In four of the six analogue pairs evaluated, it was the *trans*-R^3 analogues that exhibited higher CL_{int} values with *trans*-R^3 analogues **12a** and **12c** showing lower intrinsic clearance than their *cis*-R^4 comparators. Clearance appeared to be CYP mediated in all cases, with the possible exception of **2c**, where chemical instability or non-CYP-mediated clearance was implicated. The kinetic solubilities of arterolane

DOI: 10.1021/acs.jmedchem.7b00699
J. Med. Chem. XXXX, XXX, XXX−XXX

Scheme 4. Stereocontrolled Synthesis of 1,2,4-Trioxolane Analogues 12a–k[a]

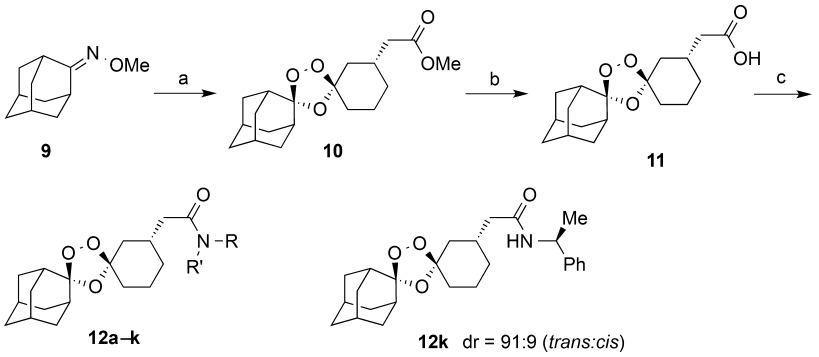

[a]Reagents and conditions: (a) 0.5 equiv of 7, O_3, CCl_4, 0 °C, 3 h, 95%; (b) NaOH, EtOH/H_2O, 50 °C, 4 h, 95%; (c) ethyl chloroformate, Et_3N, CH_2Cl_2, −10 °C, 75 min; R(R′)NH, CH_2Cl_2, −10 °C to rt, 2–24 h, 68–95%.

Chart 1. In Vitro Activity of Trioxolanes 12a–j and 2a–j against W2 *P. falciparum* Parasites[a]

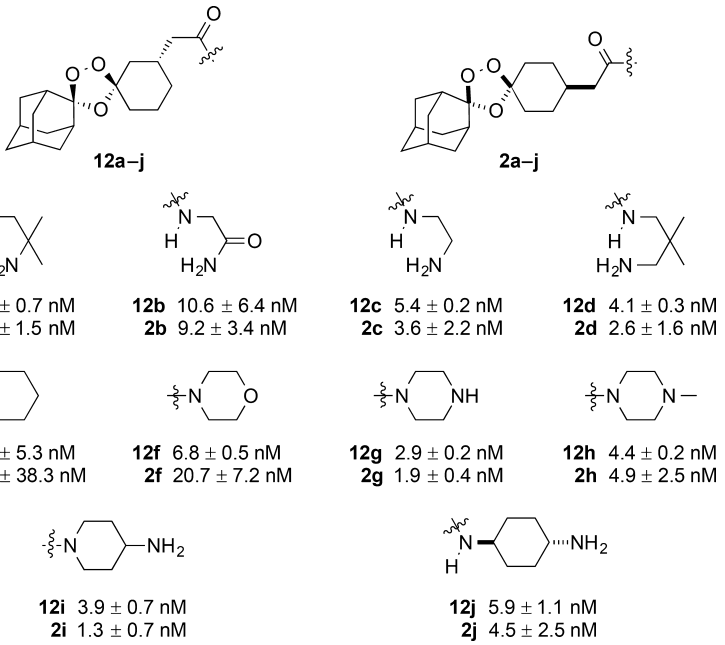

[a]In vitro activity of **12a–j** and **2a–j** against W2 *P. falciparum* parasites (EC_{50} ± SEM). Reported EC_{50} values are the means of three determinations ± SEM

(**2a**) and its regioisomer **12a** were evaluated and found to be comparable. Overall, the in vitro ADME data suggested that *trans*-R^3 analogues were suitable for evaluation in animals and that specific analogues might be differentiated from their comparators in vivo.

The suppressive 4-day "Peters test"[27] involving *P. berghei* infected mice provides a convenient and cost-effective means to assess the overall in vivo performance of preclinical antimalarials. Thus, groups of five *P. berghei* infected female Swiss Webster mice were treated via oral gavage with four daily (QD) doses of either **2a** (as the tosylate salt), regioisomeric comparator **12a** (both tosylate and free base), or chloroquine control (Table 2). Mice were followed for 30 days and judged to have been cured of the infection based on the lack of detectable parasitemia at the end of the study. In this initial study, *trans*-R^3 analogue **12a** as either tosylate salt or free base exhibited efficacy comparable to arterolane tosylate, producing cures in all five animals.

This result indicated that **12a** was orally absorbed and achieved systemic exposure sufficient to produce a robust pharmacodynamic response. Prior to evaluating additional *trans*-R^3 analogues, we sought to determine the 50% curative dose for both **12a** and **2a** in this model and use this dose as a benchmark for future studies. Thus, compounds **12a** and **2a** (both as free bases) were administered to mice over 4 days at doses of 10, 6, 4, or 1 mg kg^{-1} day^{-1}, and survival and parasitemia were monitored until 30 days postinfection. This study revealed a clear dose–efficacy relationship and allowed us to estimate 50% curative dose (PD_{50}) values of ∼6 mg kg^{-1} day^{-1} for **12a** and ∼4 mg kg^{-1} day^{-1} for **2a** (Table 3). With the *trans*-R^3 chemotype validated in vivo and a relatively stringent dose/efficacy benchmark established, we set out to more broadly evaluate the matched pairs of regioisomeric analogues in animals.

As noted previously, the *cis*-R^4 amide comparators were selected in part based on in vivo efficacy data in patents and other reports[28] from the Vennerstrom group. Therefore, all nine *cis*-R^4 analogues were expected to have good in vivo prospects, whereas the in vivo performance of the *trans*-R^3 comparators was less certain. In the next study then, all 20 test compounds (**2a–j** and

DOI: 10.1021/acs.jmedchem.7b00699
J. Med. Chem. XXXX, XXX, XXX–XXX

Table 1. In Vitro ADME Data for Selected Trioxolane Analogues and Controls

cmpd	$T_{1/2}$ (min)[a]	CL_{int}[b]	$T_{1/2}$ (min) no NADPH	solubility (μM)[c]
2a	128	5.4	stable	433
12a	169	4.1	stable	429
2b	124	5.6	stable	
12b	37.3	18.6	stable	
2c	64.2	10.8	70	
12c	84.5	8.2	136	
2d	161	4.3	stable	
12d	64.2	10.8	stable	
2g	48.1	14.4	88.9	
12g	25.5	27.2	stable	
2i	277	2.5	stable	
12i	84.5	8.2	stable	
midazolam	1.65	420		
diclofenac	55.5	12.5		
amiodarone				<3
testosterone				315

[a]Half-life when incubated with mouse liver microsomes. [b]Clearance in units of μL min^{-1} mg^{-1} of protein calculated as CL_{int} = ln(2)*1000/$T_{1/2}$/protein concentration, where protein concentration is in mg/mL; midazolam and diclofenac served as controls. [c]Kinetic solubility in PBS (pH 7.4) at a final DMSO concentraion of 5% as an average of three determinations; amiodarone and testosterone served as controls.

Table 2. In Vivo Efficacy of Trioxolanes 12a and 2a and Controls in *P. berghei*-Infected Mice Treated for 4 Days[a]

treatment	salt form	dose (mg kg^{-1} day^{-1})	mice cured[b] (%)
2a	tosylate	13.6	100
12a	tosylate	13.6	100
12a	free base	9.5	100
chloroquine		30	80
vehicle treated			0
untreated			0

[a]Beginning 1 h after infection, cohorts of five *P. berghei*-infected female Swiss Webster mice were treated once a day for 4 days by oral gavage. [b]Mice were considered cured if there was no detectable parasitemia at 30 days postinfection.

Table 3. In Vivo Efficacy of 12a and 2a in *P. berghei*-Infected Mice Following Four Daily Doses[a]

treatment	dose[a] (mg kg^{-1} day^{-1})	mice cured[b] (%)
12a	1	0
	4	0
	6	60
	10	100
2a	1	0
	4	80
	6	100
	10	100
vehicle		0
untreated		0

[a]Beginning 1 h after infection, cohorts of five *P. berghei*-infected female Swiss Webster mice were treated once a day for 4 days by oral gavage at the indicated daily dose. [b]Mice were considered cured if there was no detectable parasitemia at 30 days postinfection.

12a–**j**) were evaluated under 4 and 6 mg/kg daily dosing protocols in groups of five Swiss Webster mice. Controls **12a** and **2a** again showed good efficacy at these low doses with analogue **12a** marginally more effective than **2a** in this study (Table 4).

Table 4. In Vivo Efficacy of Matched Analogue Pairs in *P. berghei*-Infected Mice[a]

compd	dose (mg kg^{-1} day^{-1})	mice cured[b] (%)
12a	4	60
	6	100
2a	4	20
	6	80
12b	4	0
	6	0
2b	4	0
	6	0
12c	4	100
	6	100
2c	4	0
	6	20
12d	4	0
	6	0
2d	4	40
	6	100
12e	4	0
	6	0
2e	4	0
	6	0
12f	4	0
	6	0
2f	4	0
	6	0
12g	4	0
	6	20
2g	4	100
	6	100
12h	4	0
	6	0
2h	4	0
	6	0
12i	4	100
	6	80
2i	4	100
	6	100
12j	4	60
	6	100
2j	4	80
	6	80
chloroquine	30	40
vehicle		0

[a]Beginning 1 h after infection, cohorts of five *P. berghei*-infected female Swiss Webster mice were treated once a day for 4 days by oral gavage. [b]Mice were considered cured if there was no detectable parasitemia at 30 days postinfection.

Among the other nine analogue pairs, four pairs failed to cure any mice at either dosing level. These analogues included the glycinamide (**12b** and **2b**), piperidine (**12e** and **2e**), morpholine (**12f** and **2f**), and *N*-methyl piperazine (**12h** and **2h**) analogues. Interestingly, whereas the piperidine and piperazine analogues failed in these studies, the structurally very similar 4-amino-piperidine derivatives **2i** and **12i** were among the most efficacious analogues examined, curing all animals at the lowest dose of 4 mg kg^{-1} day^{-1} and proving superior to **12a** and **2a**. This finding

DOI: 10.1021/acs.jmedchem.7b00699
J. Med. Chem. XXXX, XXX, XXX−XXX

regarding **2i** is consistent with a previous report[28] demonstrating the superiority of **2i** over **2a** in a similar murine model with 3 days oral dosing at 3 mg/kg. Thus, for many of the analogue pairs, in vivo efficacy seemed to track between the *cis*-R^4 and *trans*-R^3 comparators.

Of greatest interest were those analogue pairs for which in vivo efficacy varied between the *trans*-R^3 and *cis*-R^4 comparators. Most strikingly, *cis*-R^4 analogues **2d** and **2g** were fully effective at 6 mg kg^{-1} day^{-1}, whereas the analogous *trans*-R^3 comparators **12d** and **12g** failed entirely or were minimally effective (Table 4). In the case of the analogue pair **12c** and **2c**, however, it was the novel *trans*-R^3 analogue **12c** that produced full cure at either dose, whereas the *cis*-R^4 derivative **2c** was essentially ineffective. Thus, regioisomeric trioxolane analogues can in some cases exhibit starkly different efficacy in vivo despite having similar intrinsic potency against cultured parasites. These results confirmed our hopes that *trans*-R^3 substitution might offer new avenues for the optimization of PK/PD properties in preclinical 1,2,4-trioxolanes. In the case of analogue pairs **12c** and **2c**, **12d** and **2d**, and **12g** and **2g**, CL_{int} values from the mouse liver microsome assay correctly predicted the superior analogue in each pair (compare Tables 1 and 4). However, the magnitude of differences in CL_{int} values seems insufficient to fully explain the differences observed, nor do the CL_{int} values alone explain the failure of **12b** and **2b**. It appears that additional in vivo PK/PD studies will be required to fully understand the relative merits of 3″ and 4″ substitution within the context of specific side chain types.

Given that the novel *trans*-R^3 analogues **12c** and **12i** demonstrated complete cures at 4 mg kg^{-1} day^{-1}, we next explored whether even lower doses of these agents might be effective in mice. Although **12c** and **12i** again cured all animals at a 4 mg kg^{-1} day^{-1} dose, neither produced cures with reduced doses of 2, 1, or 0.5 mg kg^{-1} day^{-1} (Table 5). We next asked whether a full 4 days of treatment at 4 mg kg^{-1} day^{-1} was necessary to achieve cures with **12c** and **12i**, cognizant that current antimalarial target product profiles seek agents with shortened dosing regimens. When **12c** and **12i** were administered at 4 mg/kg for 4, 3, 2, or 1 day, a predictable decline in efficacy with the number of doses was observed (Table 6). Thus, both compounds were again fully effective at four daily doses of 4 mg/kg, and **12i** was shown to be superior to **12c** with three daily doses of 4 mg/kg (60 vs 20% of animals cured for **12i** and **12c**, respectively). Neither compound was curative with one or two daily doses of 4 mg/kg, although under these regimens mouse survival was extended ∼3−6 days compared to that of vehicle-treated control animals.

Table 5. In Vivo Efficacy of 12c and 12i in *P. berghei*-Infected Mice at Various Dosing Levels[a]

compd	dose (mg kg^{-1} day^{-1})	mice cured[b] (%)
12c	0.5	0
	1	0
	2	0
	4	100
12i	0.5	0
	1	0
	2	0
	4	100

[a]Beginning 1 h after infection, cohorts of five *P. berghei*-infected female Swiss Webster mice were treated once a day for 4 days by oral gavage. [b]Mice were considered cured if there was no detectable parasitemia at 30 days postinfection.

Table 6. In Vivo Efficacy of 12c and 12i in *P. berghei*-Infected Mice with Less Frequent Dosing[a]

compd	dose (mg/kg)	number of doses	mice cured[b] (%)
12c	4	4	100
	4	3	20
	4	2	0
	4	1	0
12i	4	4	100
	4	3	60
	4	2	0
	4	1	0

[a]Beginning 1 h after infection, cohorts of five *P. berghei* infected female Swiss Webster mice were treated once a day by oral gavage for either four, three, two, or 1 day as shown above. [b]Mice were considered cured if there was no detectable parasitemia at 30 days postinfection.

In a final in vivo study, we evaluated the efficacy of **12c** and **12i** following a single dose of 40 or 80 mg/kg or two doses of 40 mg/kg (Table 7). We included as a positive control in this study artefenomel (**3**),[4,29] which is known to be highly effective in these models. Indeed, a single dose of **3** was remarkably effective, curing all animals at both doses examined. Although the new analogues **12c** and **12i** were completely effective with two doses of 40 mg kg^{-1} day^{-1}, a single dose of 40 mg/kg was only partially effective for **12i** and ineffective for **12c**. Both compounds were partially effective with a single 80 mg/kg dose and again **12i** proved superior to **12c** (60 vs 20% cures). Thus, multiple PD studies consistently revealed analogue **12i** to be the most promising of the novel *trans*-3″ analogues explored herein, although it was inferior to artefenomel (**3**), which has demonstrated[4] single-dose cures at 20 mg/kg in similar models.

Table 7. Efficacy of 12c, 12i, and Artefenomel in *P. berghei*-Infected Mice Following a Single or Repeated Dose[a]

compd	dose (mg/kg)	number of doses	mice cured[b] (%)
3 (artefenomel)	40	1	100
	80	1	100
12c	40	2	100
	40	1	0
	80	1	20
12i	40	2	100
	40	1	20
	80	1	60

[a]Beginning 1 h after infection, cohorts of five *P. berghei*-infected female Swiss Webster mice were treated by oral gavage for either 1 or 2 days at the indicated dose. [b]Mice were considered cured if there was no detectable parasitemia at 30 days postinfection.

CONCLUSIONS

The unusual Fe(II)-dependent pharmacology of antimalarial 1,2,4-trioxolanes necessitates an equally unusual approach to their optimization, namely, one that recognizes and exploits the strong connection between conformational dynamics, chemical reactivity, and antiparasitic effects.[16] Clinical experience with **2a** and **3** perfectly illustrates this point. Thus, early clinical studies of **2a** revealed inferior drug exposure and half-life in malaria patients when compared to healthy volunteers. This effect was traced to reaction of **2a** with endogenous Fe(II) sources in infected

DOI: 10.1021/acs.jmedchem.7b00699
J. Med. Chem. XXXX, XXX, XXX−XXX

individuals. Nevertheless, by modifying the nature of the *cis*-4″ side chain, a superior drug candidate (**3**) with much improved Fe(II) stability and in vivo PK properties was identified.[4] Now, an improved understanding[13−15] of how emergent K13 mutant parasites escape endoperoxide exposure provides rationale for identifying new endoperoxides that more rapidly kill *P. falciparum* K13 mutant ring forms while retaining stability toward endogenous Fe(II) sources in the host. The result of just such an effort focused on a tetraoxane chemotype has appeared very recently.[30]

Here, we present the first systematic study comparing the canonical *cis*-4″-substituted pharmacophore of **2a** and **3** with regioisomeric *trans*-3″-substituted analogues. On the basis of their in vitro and in vivo properties, we conclude that the *trans*-3″ side chain modulates peroxide reactivity in a pharmacologically relevant regime as hoped. In this preliminary study, we examined just ten side chains employed previously in *cis*-4″ analogues. Even with this limited survey, two novel analogues were identified that exhibited in vivo properties superior to **2a** in the *P. berghei* model, and one that afforded single-dose cures at higher doses. The ultimate potential of the new 3″-substituted chemotype will only be revealed with the examination of a more diverse set of side chains, and in particular, those designed to exploit steric and conformational effects unique to this substitution pattern. Efforts in this direction are well underway in our laboratories and will be described in due course.

EXPERIMENTAL SECTION

Known compounds were prepared according to literature procedures as cited in the main text. The syntheses of new compounds **12a−k** are described in the Supporting Information. All compounds tested in parasites or mice were judged to be of >95% purity as assessed using a Waters Micromass ZQ 4000 equipped with Waters 2795 Separation Module, Waters 2996 Photodiode Array Detector (254 nm), and Waters 2424 ELS detector. Separations were carried out with an XBridge BEH C18, 3.5 μm, 4.6 × 20 mm column, at ambient temperature (unregulated) using a mobile phase of water−methanol containing a constant 0.10% formic acid.

***Plasmodium falciparum* EC_{50} Determinations.** The growth inhibition assay for *P. falciparum* was conducted as described previously[31] with minor modifications. Briefly, *Plasmodium falciparum* strain W2 synchronized ring-stage parasites were cultured in human red blood cells in 96-well flat bottom culture plates at 37 °C, adjusted to 1% parasitemia and 2% hematocrit under an atmosphere of 3% O_2, 5% CO_2, and 91% N_2 in a final volume of 0.1 mL per well in RPMI-1640 media supplemented with 0.5% Albumax, 2 mM L-glutamine, and 100 mM hypoxanthine in the presence of various concentrations of inhibitors. Tested compounds were serially diluted 1:3 in the range 10000−4.6 nM (or 1000−0.006 nM for more potent analogues) with a maximum DMSO concentration of 0.1%. Following 48 h of incubation, the cells were fixed by adding 0.1 mL of 2% formaldehyde in phosphate buffered saline, pH 7.4 (PBS). Parasite growth was evaluated by flow cytometry on a FACsort (Becton Dickinson) equipped with AMS-1 loader (Cytek Development) after staining with 1 nM of the DNA dye YOYO-1 (Molecular Probes) in 100 mM NH_4Cl and 0.1% Triton x-100 in 0.8% NaCl. Parasitemias were determined from dot plots (forward scatter vs fluorescence) using CELLQUEST software (Becton Dickinson). EC_{50} values for growth inhibition were determined from plots of percentage control parasitemia over inhibitor concentration using GraphPad Prism software.

***Plasmodium berghei* Mouse Malaria Model.** Female Swiss Webster Mice (average of 20 g body weight) were infected intraperitoneally with 10^6 *Plasmodium berghei*-infected erythrocytes collected from a previously infected mouse. Beginning 1 h after inoculation, the mice were treated once daily by oral gavage for 1−4 days with 100 μL of solution of test compound formulated in a vehicle comprised of 10% DMSO, 40% of a 20% solution of 2-hydroxypropyl-β-cyclodextrin in water, and 50% PEG400. There were five mice in each test arm. Infections were monitored by daily microscopic evaluation of Giemsa-stained blood smears starting on day 7. Parasitemia were determined by counting the number of infected and uninfected erythrocytes. Body weight was measured over the course of the treatment. Mice were euthanized when parasitemia exceeded 50% or when weight loss of more than 15% occurred. Animal survival and morbidity were closely monitored for up to 30 days postinfection when the experiment was terminated.

ASSOCIATED CONTENT

Supporting Information

The Supporting Information is available free of charge on the ACS Publications website at DOI: 10.1021/acs.jmedchem.7b00699.

Synthetic procedures and compound characterization for new compounds (PDF)
Molecular formula strings (CSV)

AUTHOR INFORMATION

Corresponding Author

*Phone: 415-514-9698; fax: 415-514-4507; e-mail: adam.renslo@ucsf.edu.

ORCID

Adam R. Renslo: 0000-0002-1240-2846

Author Contributions

B.R.B., J.G., and A.R.R conceived experiments. B.R.B. devised synthetic routes and synthesized compounds. B.R.B. and J.G. acquired data. All authors analyzed data. A.R.R. supervised the project. B.R.B. and A.R.R wrote the manuscript. All authors reviewed, edited, and commented on the manuscript. All authors have given approval to the final version of the manuscript.

Notes

The authors declare no competing financial interest.

ACKNOWLEDGMENTS

A.R.R. acknowledges funding from the US National Institutes of Health (R01 Grant AI105106). We thank Prof. J. Vennerstrom for the generous gift of intermediate **4**.

ABBREVIATIONS USED

DHA, dihydroartemisinin; ACT, artemisinins combination therapy; WHO, World Health Organization; PK, pharmacokinetics; PD, pharmacodynamics; CL_{int}, intrinsic clearance; MLM, mouse liver microsome assay; QD, once-daily dosing

REFERENCES

(1) Posner, G. H.; Oh, C. H. A Regiospecifically Oxygen-18 Labeled 1, 2, 4-Trioxane: A Simple Chemical Model System To Probe the Mechanism(s) for the Antimalarial Activity of Artemisinin (Qinghaosu). *J. Am. Chem. Soc.* **1992**, *114*, 8328−8329.

(2) Posner, G. H.; Oh, C. H.; Wang, D.; Gerena, L.; Milhous, W. K.; Meshnick, S. R.; Asawamahasadka, W. Mechanism-Based Design, Synthesis and in Vitro Antimalarial Testing of New 4-Methylated Trioxanes Structurally Related to Artemisinin: The Importance of a Carbon-Centered Radical for Antimalarial Activity. *J. Med. Chem.* **1994**, *37*, 1256−1258.

(3) Vennerstrom, J. L.; Arbe-Barnes, S.; Brun, R.; Charman, S. A.; Chiu, F. C. K.; Chollet, J.; Dong, Y.; Dorn, A.; Hunziker, D.; Matile, H.; McIntosh, K.; Padmanilayam, M.; Santo Tomas, J.; Scheurer, C.; Scorneaux, B.; Tang, Y.; Urwyler, H.; Wittlin, S.; Charman, W. N. Identification of an Antimalarial Synthetic Trioxolane Drug Development Candidate. *Nature* **2004**, *430*, 900−904.

DOI: 10.1021/acs.jmedchem.7b00699
J. Med. Chem. XXXX, XXX, XXX−XXX

(4) Charman, S. A.; Arbe-Barnes, S.; Bathurst, I. C.; Brun, R.; Campbell, M.; Charman, W. N.; Chiu, F. C. K.; Chollet, J.; Craft, J. C.; Creek, D. J.; Dong, Y.; Matile, H.; Maurer, M.; Morizzi, J.; Nguyen, T.; Papastogiannidis, P.; Scheurer, C.; Shackleford, D. M.; Sriraghavan, K.; Stingelin, L.; Tang, Y.; Urwyler, H.; Wang, X.; White, K. L.; Wittlin, S.; Zhou, L.; Vennerstrom, J. L. Synthetic Ozonide Drug Candidate OZ439 Offers New Hope for a Single-Dose Cure of Uncomplicated Malaria. *Proc. Natl. Acad. Sci. U. S. A.* **2011**, *108*, 4400−4405.
(5) Moehrle, J. J.; Duparc, S.; Siethoff, C.; van Giersbergen, P. L. M.; Craft, J. C.; Arbe-Barnes, S.; Charman, S. A.; Gutierrez, M.; Wittlin, S.; Vennerstrom, J. L. First-in-Man Safety and Pharmacokinetics of Synthetic Ozonide OZ439 Demonstrates an Improved Exposure Profile Relative to Other Peroxide Antimalarials. *Br. J. Clin. Pharmacol.* **2013**, *75*, 524−537.
(6) Phyo, A. P.; Jittamala, P.; Nosten, F. H.; Pukrittayakamee, S.; Imwong, M.; White, N. J.; Duparc, S.; Macintyre, F.; Baker, M.; Möhrle, J. J. Antimalarial Activity of Artefenomel (OZ439), a Novel Synthetic Antimalarial Endoperoxide, in Patients with Plasmodium Falciparum and Plasmodium Vivax Malaria: An Open-Label Phase 2 Trial. *Lancet Infect. Dis.* **2016**, *16*, 61−69.
(7) Ismail, H. M.; Barton, V. E.; Panchana, M.; Charoensutthivarakul, S.; Biagini, G. A.; Ward, S. A.; O'Neill, P. M. A Click Chemistry-Based Proteomic Approach Reveals That 1,2,4-Trioxolane and Artemisinin Antimalarials Share a Common Protein Alkylation Profile. *Angew. Chem.* **2016**, *128*, 6511−6515.
(8) Ismail, H. M.; Barton, V.; Phanchana, M.; Charoensutthivarakul, S.; Wong, M. H. L.; Hemingway, J.; Biagini, G. A.; O'Neill, P. M.; Ward, S. A. Artemisinin Activity-Based Probes Identify Multiple Molecular Targets within the Asexual Stage of the Malaria Parasites Plasmodium Falciparum 3D7. *Proc. Natl. Acad. Sci. U. S. A.* **2016**, *113*, 2080−2085.
(9) Wang, J.; Zhang, C.-J.; Chia, W. N.; Loh, C. C. Y.; Li, Z.; Lee, Y. M.; He, Y.; Yuan, L.-X.; Lim, T. K.; Liu, M.; Liew, C. X.; Lee, Y. Q.; Zhang, J.; Lu, N.; Lim, C. T.; Hua, Z.-C.; Liu, B.; Shen, H.-M.; Tan, K. S. W.; Lin, Q. Haem-Activated Promiscuous Targeting of Artemisinin in Plasmodium Falciparum. *Nat. Commun.* **2015**, *6*, 10111.
(10) Amaratunga, C.; Lim, P.; Suon, S.; Sreng, S.; Mao, S.; Sopha, C.; Sam, B.; Dek, D.; Try, V.; Amato, R.; Blessborn, D.; Song, L.; Tullo, G. S.; Fay, M. P.; Anderson, J. M.; Tarning, J.; Fairhurst, R. M. Dihydroartemisinin−Piperaquine Resistance in Plasmodium Falciparum Malaria in Cambodia: A Multisite Prospective Cohort Study. *Lancet Infect. Dis.* **2016**, *16*, 357−365.
(11) Ariey, F.; Witkowski, B.; Amaratunga, C.; Beghain, J.; Langlois, A.-C.; Khim, N.; Kim, S.; Duru, V.; Bouchier, C.; Ma, L.; Lim, P.; Leang, R.; Duong, S.; Sreng, S.; Suon, S.; Chuor, C. M.; Bout, D. M.; Ménard, S.; Rogers, W. O.; Genton, B.; Fandeur, T.; Miotto, O.; Ringwald, P.; Le Bras, J.; Berry, A.; Barale, J.-C.; Fairhurst, R. M.; Benoit-Vical, F.; Mercereau-Puijalon, O.; Ménard, D. A Molecular Marker of Artemisinin-Resistant Plasmodium Falciparum Malaria. *Nature* **2014**, *505*, 50−55.
(12) Dogovski, C.; Xie, S. C.; Burgio, G.; Bridgford, J.; Mok, S.; McCaw, J. M.; Chotivanich, K.; Kenny, S.; Gnädig, N.; Straimer, J.; Bozdech, Z.; Fidock, D. A.; Simpson, J. A.; Dondorp, A. M.; Foote, S.; Klonis, N.; Tilley, L. Targeting the Cell Stress Response of Plasmodium Falciparum to Overcome Artemisinin Resistance. *PLoS Biol.* **2015**, *13*, e1002132.
(13) Yang, T.; Xie, S. C.; Cao, P.; Giannangelo, C.; McCaw, J.; Creek, D. J.; Charman, S. A.; Klonis, N.; Tilley, L. Comparison of the Exposure Time Dependence of the Activities of Synthetic Ozonide Antimalarials and Dihydroartemisinin against K13 Wild-Type and Mutant Plasmodium Falciparum Strains. *Antimicrob. Agents Chemother.* **2016**, *60*, 4501−4510.
(14) Straimer, J.; Gnädig, N. F.; Stokes, B. H.; Ehrenberger, M.; Crane, A. A.; Fidock, D. A. *Plasmodium falciparum* K13 Mutations Differentially Impact Ozonide Susceptibility and Parasite Fitness. *mBio* **2017**, *8*, e00172−17.
(15) Baumgärtner, F.; Jourdan, J.; Scheurer, C.; Blasco, B.; Campo, B.; Mäser, P.; Wittlin, S. In vitro activity of anti-malarial ozonides against an artemisinin-resistant isolate. *Malar. J.* **2017**, *16*, 45.
(16) Creek, D.; Charman, W.; Chiu, F. C. K.; Prankerd, R. J.; McCullough, K. J.; Dong, Y.; Vennerstrom, J. L.; Charman, S. A. Iron-Mediated Degradation Kinetics of Substituted Dispiro-1,2,4-Trioxolane Antimalarials. *J. Pharm. Sci.* **2007**, *96*, 2945−2956.
(17) Zhao, Q.; Vargas, M.; Dong, Y.; Zhou, L.; Wang, X.; Sriraghavan, K.; Keiser, J.; Vennerstrom, J. L. Structure-Activity Relationship of an Ozonide Carboxylic Acid (OZ78) Against Fasciola Hepatica. *J. Med. Chem.* **2010**, *53*, 4223−4233.
(18) Vennerstrom, J. L.; Dong, Y.; Chollet, J.; Matile, H.; Padmanilayam, M.; Tang, Y.; Charman, W. N. Spiro and Dispiro 1,2,4-trioxolane Antimalarials. U.S. Patent 2004/0039008 A1, February 26, 2004.
(19) Yadav, G. C.; Dorwal, H. N.; Valavala, S.; Sharma, V. K. A Process for the Preparation of Spiro and Dispiro 1,2,4-trioxolane Antimalarials. PCT WO 2007/138435 A2, December 6, 2007.
(20) Fontaine, S. D.; Dipasquale, A. G.; Renslo, A. R. Efficient and Stereocontrolled Synthesis of 1,2,4-Trioxolanes Useful for Ferrous Iron-Dependent Drug Delivery. *Org. Lett.* **2014**, *16*, 5776−5779.
(21) Shibasaki, M.; Sasai, H.; Arai, T. Asymmetric Catalysis with Heterobimetallic Compounds. *Angew. Chem., Int. Ed. Engl.* **1997**, *36*, 1236−1256.
(22) Shimizu, S.; Ohori, K.; Arai, T.; Sasai, H.; Shibasaki, M. A Catalytic Asymmetric Synthesis of Tubifolidine. *J. Org. Chem.* **1998**, *63*, 7547−7551.
(23) Xu, Y.; Ohori, K.; Ohshima, T.; Shibasaki, M. A. A Practical Large-Scale Synthesis of Enantiomerically Pure 3-[Bis(methoxycarbonyl)-methyl]cyclohexanone via Catalytic Asymmetric Michael Reaction. *Tetrahedron* **2002**, *58*, 2585−2588.
(24) Tzvetkov, N. T.; Schmoldt, P.; Neumann, B.; Stammler, H.-G.; Mattay, J. Synthesis of Optically Active (1R,4S,6S)-6-hydroxybicyclo[2.2.2]octan-2-One. *Tetrahedron: Asymmetry* **2006**, *17*, 993−998.
(25) Riguet, E. Novel Guanidinyl Pyrrolidine Salt-Based Bifunctional Organocatalysts: Application in Asymmetric Conjugate Addition of Malonates to Enones. *Tetrahedron Lett.* **2009**, *50*, 4283−4285.
(26) Wascholowski, V.; Knudsen, K. R.; Mitchell, C. E. T.; Ley, S. V. A General Organocatalytic Enantioselective Malonate Addition to α,β-Unsaturated Enones. *Chem. - Eur. J.* **2008**, *14*, 6155−6165.
(27) Peters, W. In *Chemotherapy and Drug Resistance in Malaria*; Academic Press, Inc.: New York, NY, 1987; pp 145−273.
(28) Dong, Y.; Wittlin, S.; Sriraghavan, K.; Chollet, J.; Charman, S. A.; Charman, W. N.; Scheurer, C.; Urwyler, H.; Santo Tomas, J.; Snyder, C.; Creek, D. J.; Morizzi, J.; Koltun, M.; Matile, H.; Wang, X.; Padmanilayam, M.; Tang, Y.; Dorn, A.; Brun, R.; Vennerstrom, J. L. The Structure-Activity Relationship of the Antimalarial Ozonide Arterolane (OZ277). *J. Med. Chem.* **2010**, *53*, 481−491.
(29) Vennerstrom, J. L.; Dong, Y.; Charman, S. A.; Wittlin, S.; Chollet, J.; Creek, D. J.; Wang, X.; Sriraghavan, K.; Zhou, L.; Matile, H.; Charman, W. N. Dispiro 1,2,4-trioxolane Antimalarials. PCT WO 2009/058859 A2, May 7, 2009.
(30) O'Neill, P. M.; Amewu, R. K.; Charman, S. A.; Sabbani, S.; Gnädig, N. F.; Straimer, J.; Fidock, D. A.; Shore, E. R.; Roberts, N. L.; Wong, M. H.-L.; Hong, W. D.; Pidathala, C.; Riley, C.; Murphy, B.; Aljayyoussi, G.; Gamo, F. J.; Sanz, L.; Rodrigues, J.; Cortes, C. G.; Herreros, E.; Angulo-Barturén, I.; Jiménez-Díaz, M. B.; Bazaga, S. F.; Martínez-Martínez, M. S.; Campo, B.; Sharma, R.; Ryan, E.; Shackleford, D. M.; Campbell, S.; Smith, D. A.; Wirjanata, G.; Noviyanti, R.; Price, R. N.; Marfurt, J.; Palmer, M. J.; Copple, I. M.; Mercer, A. E.; Ruecker, A.; Delves, M. J.; Sinden, R. E.; Siegl, P.; Davies, J.; Rochford, R.; Kocken, C. H. M.; Zeeman, A.-M.; Nixon, G. L.; Biagini, G. A.; Ward, S. A. A Tetraoxane-Based Antimalarial Drug Candidate That Overcomes PfK13-C580Y Dependent Artemisinin Resistance. *Nat. Commun.* **2017**, *8*, 15159.
(31) Sijwali, P. S.; Rosenthal, P. J. Gene Disruption Confirms a Critical Role for the Cysteine Protease Falcipain-2 in Hemoglobin Hydrolysis by Plasmodium Falciparum. *Proc. Natl. Acad. Sci. U. S. A.* **2004**, *101*, 4384−4389.

DOI: 10.1021/acs.jmedchem.7b00699
J. Med. Chem. XXXX, XXX, XXX−XXX